Available online at www.sciencedirect.com
ScienceDirect
Journal of Molecular Catalysis A: Chemical 278 (2007) 53–63
JOURNAL OF MOLECULAR CATALYSIS A: CHEMICAL
www.elsevier.com/locate/molcata

A new way for deNO$_x$ catalyst preparation: Direct incorporation of 12-tungstophosphoric acid $H_3PW_{12}O_{40}$ and platinum into mesoporous molecular sieves material

Hussein Hamad [a,b,*], Michel Soulard [a], Bénédicte Lebeau [a], Joël Patarin [a], Tayssir Hamieh [b], Joumana Toufaily [b], Hakim Mahzoul [c]

[a] *Laboratoire de Matériaux à Porosité Contrôlée, UMR 7016, ENSCMu, UHA, 3 rue Alfred Werner, 68093 Mulhouse Cedex, France*
[b] *Laboratoire de Chimie Analytique, Matériaux, Surfaces et Interfaces, Faculté des Sciences, Université Libanaise, Hadeth, Beyrouth, Lebanon*
[c] *Laboratoire Gestion des Risques et Environnement, EA 2334, UHA, 25 rue de Chemnitz, 68200 Mulhouse, France*

Received 22 May 2007; received in revised form 7 August 2007; accepted 24 August 2007
Available online 1 September 2007

Abstract

Direct incorporation of platinum (Pt) and 12-tungstophosphoric acid $H_3PW_{12}O_{40}$ (HPW) into mesoporous MSU-type silica was achieved by using a mixture of cationic and non-ionic surfactants, such as cetyltrimethylammonium ($C_{16}TMA^+$) and Triton (TX-100). Various amounts of Pt (0.3–7 wt%) and HPW (9–49 wt%) were incorporated and the obtained materials were characterized by X-ray diffraction (XRD), chemical and thermal (TG–DTA) analyses, electron microscopies (SEM, TEM), N_2 adsorption–desorption measurements, and solid state ^{31}P NMR spectroscopy. The catalytic activity of the calcined silica-based mesoporous molecular sieves containing tungstophosphoric acid (HPW), platinum and platinum–tungstophosphoric acid (Pt/HPW) for NO_x reduction with propene was investigated in the presence of oxygen. Samples which contain small amounts of Pt and moderate loadings of HPW were found the most active (up to 97% at 250 °C and for 1 vol.% O_2).

Keywords: Mesoporous silica-based material; Direct incorporation; Platinum; Tungstophosphoric acid; NO_x reduction

1. Introduction

Since their discovery in the early 1990s, the organized mesoporous molecular sieves of the M41S family [1] have been intensively modified to generate materials with catalytic properties. Thus, the introduction of different elements such as Al, Ti, Zr into organized mesoporous siliceous structures has been reported [2–4]. However, compared to zeolites, the acid properties of aluminum-containing M41S materials are lower and similar to those observed for amorphous silica–alumina [3,5]. Another route was explored such as the preparation of metal supported MCM-41and MCM-48 silica type materials [6–9]. Indeed, the high surface area of these mesoporous materials appears to be very promising for a good dispersion of the active metal component and consequently for an outstanding catalytic activity [9–11]. Junges et al. [12] have reported an interesting approach for the preparation of metal supported mesoporous materials by using different platinum sources introduced directly in the synthesis gel of MCM-41. By this way up to 5 wt% of Pt could be incorporated into the solids without any distortion of the ordered MCM-41 structure.

On the other hand, heteropolyacids (HPAs) with the Keggin structure are widely used as acid catalysts, due to their very strong Brönsted acidity [13–15]. The tungsten addenda atoms present in heteropolyacids exhibit strong acidity, high thermal stability and oxidation properties [13], which allow their use as catalysts in various reactions at moderate temperatures [16]. Moreover, the high solubility of HPAs in water and organic solvents, their quite high thermal stability in the solid state [17] and the possibility of introducing several different elements into the polyanions and counter-cations [18], have opened a new field of research in catalysis. It is well known that HPAs strongly inter-

* Corresponding author at: NanoQam (Laboratoire d'électrochimie avancée) Case postale 8888, succursale Centre-ville Montréal (Québec) H3C 3P8 Canada. Tel.: +1 514 987 3000x1433; fax: +1 514 987 4054.
E-mail addresses: hussein29@hotmail.com, hhamad@emt.inrs.ca (H. Hamad).

1381-1169/$ – see front matter © 2007 Elsevier B.V. All rights reserved.
doi:10.1016/j.molcata.2007.08.024

act with the support at low loading levels, while bulk properties of heteropolyacids prevail at higher loadings [19].

Furthermore, as mentioned by Nowińska et al., encapsulation of HPAs and transition metal complexes into the channels of mesoporous materials was used to generate stable catalysts with both acid and oxidative catalytic activity [20]. However, the anchoring of HPAs into mesoporous materials walls occurs by means of very weak interactions between the acidic proton and the silanol groups, which might explain, in some cases, the leaching of these species in liquid phase reactions.

There are many papers describing the use of mesoporous molecular sieves, such as MCM-41, as a catalyst support and the role played by their textural properties in the degree of metal dispersion and metal reduction and the corresponding effect on catalytic behavior [21]. Thus, MCM-41 materials containing metals or metallic ions, have showed outstanding activity for NO_x reduction [6,10,11], especially Pt-supported MCM-41 obtained by impregnation. Recently, Jang et al. [22] reported that the catalytic performances in NO_x reduction by Pt-impregnated MCM-41 and MCM-48 depended on the characteristics of the supports used. In addition, Jentys et al. [11] have studied the catalytic properties of MCM-41 impregnated with platinum and tungstophosphoric acid. Such an impregnation generates strong Brønsted acid sites on the solids and improves their activity. Toufaily [23] showed that the preparation of MSU-type materials under acidic medium using two types of surfactants, cetyltrimethylammonium ($C_{16}TMA^+$) and Triton (TX-100), enhance the incorporation of tungstophosphoric acid (HPW) into the pores of MSU-type materials. The addition of a cationic surfactant such as $C_{16}TMA^+$ during the synthesis might be an advantage for the incorporation of negatively charged species such as chloroplatinic and tungstophosphoric species.

In the present paper, the direct synthesis of organized mesoporous MSU-type silica modified with platinum (Pt), tungstophosphoric acid (HPW) or Pt + HPW at various loadings is described. The effect of the incorporation of Pt and HPW on the structure of the mesoporous solid was investigated. A detailed physico-chemical characterization of the obtained materials was carried out by using different techniques: namely, X-ray diffraction (XRD), elemental, SEM, TEM and TGA/DTA analyses, N_2 adsorption–desorption measurements, and solid state ^{31}P NMR spectroscopy.

The three types of prepared catalysts named HPW/MSU, Pt/MSU and Pt/HPW/MSU with various loadings in Pt and HPW were tested in catalytic deNO_x reactions with propene in the presence of variable amounts of oxygen at different temperatures.

2. Experimental

2.1. Materials

The synthesis of MSU-type silica was carried out according to the procedure developed by Toufaily [23] in which tetraethoxysilane (TEOS, purchased from Aldrich 98%) was used as silica source, cetyltrimethylammonium bromide ($C_{16}TMABr$, 96%, Fluka), polyethylene glycol-*tert*-octylphenyl-ether (TX-100, Fluka) as surfactants and sodium fluoride (NaF, Fluka) as nucleophilic catalyst for the condensation of the silica network [24]. For the Pt- and HPW-containing samples, hexahydrate chloroplatinic acid ($H_2PtCl_6{\cdot}6H_2O$, Strem Chemicals) and 12-tungstophosphoric acid ($H_3PW_{12}O_{40}$, Fluka) were used as reactants. Pure silica, Pt-, HPW- and Pt/HPW-containing samples are named MSU, Pt/MSU, HPW/MSU and Pt/HPW/MSU, respectively.

2.2. Synthesis procedures

2.2.1. Synthesis of Pt/HPW/MSU samples

The synthesis of the Pt and HPW-containing MSU-type samples was performed with the following molar composition: $1SiO_2$:0.22TX-100:0.02–0.04$C_{16}TMABr$:($0 \le m \le 0.035$) HPW:($0 \le n \le 0.04$)Pt:0.02NaF:300H_2O (see Table 1).

In a first step, 7.4 g of TX-100 and 0.41–0.82 g of $C_{16}TMABr$ were dissolved in 210 mL distilled H_2O containing 10 mL of

Table 1
Synthesis of MSU, Pt/MSU, HPW/MSU and Pt/HPW/MSU samples

Sample	Type	Composition of the starting mixture				Composition of the MSU-type samples[a]	
		HPW, x (g)	HPW/SiO_2 molar ratio, m ($\times10^{-3}$)	H_2PtCl_6, y (g)	Pt/SiO_2 molar ratio, n ($\times10^{-3}$)	wt% of HPW and (HPW/SiO_2 molar ratio, $\times10^{-3}$)	wt% of Pt and (Pt/SiO_2 molar ratio, $\times10^{-3}$)
A	MSU	0	0	0	0	0	0
B	Pt/MSU	0	0	0.20	7.3	0	1 (3)
C	Pt/MSU	0	0	1.04	38	0	7 (26)
D	HPW/MSU	1.65	9.4	0	0	9 (2.2)	0
E	HPW/MSU	3.30	20	0	0	29 (9.8)	0
F	HPW/MSU	4.00	24	0	0	38 (14.2)	0
G	Pt/HPW/MSU	1.61	9	0.19	7	13 (3)	0.5 (1.6)
H	Pt/HPW/MSU	1.50	8.5	0.19	7	20 (5)	0.4 (1.5)
I	Pt/HPW/MSU	3.00	17	0.19	7	22 (9)	0.3 (1.1)
J	Pt/HPW/MSU	5.90	34	0.36	13	49 (23)	0.8 (2)

Starting molar composition: $1SiO_2$:0.22TX-100:0.02–0.04$C_{16}TMABr$:mHPW:nHPt:0.02NaF:300H_2O.
[a] Determined by X-ray fluorescence spectroscopy.

hydrochloric acid (4 M HCl). After a clear solution was obtained, 11 g of TEOS were added and stirred until complete dissolution. This solution will be named hereafter solution 1.

In a second step, two solutions (30 mL) of (*x*) g of HPW and (*y*) g of platinic acid (see Table 1) were prepared by dissolving the corresponding reactants in acidified (HCl) distilled water. Then, the two aliquots were mixed together for 5 min at room temperature to obtain solution 2.

Finally, solution 2 was added to solution 1 and stirred for 30 min. The resulting solution was aged for 24 h at room temperature and 0.043 g of NaF was added. After complete dissolution, the solution was placed in a polyethylene bottle and heated at 60 °C for 48 h.

The obtained precipitate was filtered, washed with distilled water and dried in air at 80 °C; the template surfactant was removed by calcination under air at 385 °C for 5 h.

2.2.2. Synthesis of HPW/MSU, Pt/MSU and MSU samples

A similar procedure was used for the synthesis of the HPW/MSU and Pt/MSU samples. Two aliquots of solution 1 were prepared as described above. For the HPW-containing MSU-type silica, solution 2 was obtained by dissolving (*x*) g of HPW in 30 mL of acidified distilled water. Whereas for the Pt-containing MSU samples, solution 2 (30 mL) was prepared by dissolving (*y*) g of $H_2PtCl_6{\cdot}6H_2O$. In both cases, solution 2 was added to solution 1 and the final volume was completed to 270 mL with H_2O. The MSU sample was obtained as described above for the preparation of solution 1. The final solutions were kept 24 h at room temperature, and 0.043 g NaF was added to each of them. Then, as described before, they were introduced in polyethylene bottles and heated at 60 °C for 48 h.

2.3. Physico-chemical characterization

2.3.1. X-ray diffraction

The powder X-ray patterns were obtained with Cu Kα radiation (λ = 1.5418 Å) on a Philips PW1800 diffractometer in the 1–10° or 1–50° (2θ) range with a 0.01° step size and a 4 s step time.

2.3.2. Scanning electron microscopy

The size and the morphology of the particles were characterized with a Philips XL30 scanning electron microscope operating at a voltage of 9 kV. Prior to the SEM observations, the samples were gold coated (thickness about 20 nm) by cathodic sputtering.

2.3.3. Transmission electron microscopy

Prior to TEM analysis, the Pt- or Pt/HPW-containing samples were prepared by ultrasonic dispersion of the powder in chloroform. Then, a few drops of the suspension were deposited on the surface of a TEM grid, which was kept at room temperature for drying. The TEM experiments were performed on a Philips CM200 microscope operating at 200 kV. An image analysis software (XT Docu, Soft Imaging System Gmbh) was used to determine the average Pt particle size.

2.3.4. Nitrogen adsorption–desorption isotherms

Nitrogen adsorption–desorption measurements were performed on a Micromeritics ASAP 2010 at 77 K. Prior to the measurements, the calcined samples were outgassed at 300 °C for 12 h. The specific surface area was determined using the BET method in the relative pressure range 0.02–0.2 [25]. The mesopore-size distribution was evaluated by the BJH method from the adsorption branch of the isotherm and using a cylindrical pore model [26].

2.3.5. TGA/DTA

Thermogravimetric (TGA) and differential thermal (DTA) analyses were performed under air on a Setaram Labsys thermoanalyzer with a heating rate of 5 °C/min up to 800 °C.

2.3.6. Elemental analysis

Elemental analyses of Si, P, W, and Pt were performed by X-ray fluorescence spectroscopy using a Magix Philips spectrometer. Appropriate reference samples were used for quantitative analysis.

2.3.7. ^{31}P MAS NMR spectroscopy

^{31}P MAS NMR spectra were recorded on a Bruker DSX 400 spectrometer at frequency 161.98 MHz with a spinning rate of 8 kHz, pulse duration 3.5 μs (flip angle $\pi/2$) and repetition time of 20 s. The number of scans was 8. The chemical shifts were measured with respect to 85% H_3PO_4 as an external reference.

2.4. Catalysis set-up

The catalytic reactions were performed using a continuous flow system in a fixed bed reactor. From 1 to 1.7 g of catalyst were deposited on a quartz frit set in a vertical silica tube (internal diameter of 16 mm). The temperature was monitored through a thermocouple located in the cell close to the catalyst sample. The gas flow rate of the injected mixture was controlled by mass flow-meters (Rosemount type 8550TR) and a total flow rate equal to 50 N L h^{-1} was used at 1 atm, with a VHSV of 30,000 h^{-1}. The reaction mixture was prepared by mixing a certified analyzed gas of 300 ppm of NO in He (Soxal), 25 vol.% O_2 (Soxal), 1 vol.% propene in He (Soxal) and 99.999% He (Soxal) carrier gas. The concentration of NO_2, NO, CO_2 and CO at the reactor outlet was determined by infrared analyzers (Rosemount NGA 2000 for the first two gases and Malhiac Multor 610 for the two last ones). A by-pass line allowed calibrating the analyzers.

The experiments were performed under isothermal conditions (temperature ranging from 170 to 350 °C). At first, the samples were heated to the reaction temperature under pure He and then the carrier gas was switched to the gas mixture. At the reactor inlet, the reactive gas mixture included NO (300 ppm), C_3H_6 (900 ppm), O_2 (concentration ranging from 0.5 to 10%). The outgoing gas composition was recorded every 5 s and after obtaining a steady state regime, the NO_x conversion was calculated from the difference of NO_x concentration between the reactor inlet and outlet.

3. Results and discussion

3.1. Structural characterization

The amounts of HPW and Pt present in the MSU-type samples were determined by X-ray fluorescence spectroscopy. The results are reported in Table 1. Whatever the HPW and Pt contents in the starting mixtures, it appears clearly that the HPW and Pt loadings in the MSU-type samples are systematically lower than the expected ones. Furthermore, for approximately the same amount of Pt in the gel (molar $Pt/SiO_2 = 7 \times 10^{-3}$), the Pt loading in the solids is much larger in the absence of HPW (compare sample B with samples G, H and I in Table 1). Therefore, the amount of $(PW_{12}O_{40})^{3-}$ or $PtCl_6^{2-}$ incorporated is related to the access of acids species to the positive charge accessible of the protonated or the cationic surfactants (see below).

For the Pt/HPW-containing samples, the HPW loading seems to be more efficient than the Pt one; the incorporation yields expressed in mol% correspond to 50 and 20%, respectively.

3.1.1. Powder X-ray diffraction

The powder XRD patterns of the calcined MSU and Pt/MSU samples are reported in Fig. 1. At low angle, they display a XRD peak ($d = 44$ Å) with a broad component at $d = 23$ Å; the latter being more pronounced for the Pt-free sample. Such XRD patterns are characteristic of a MSU-X-type structure with vermicular pore geometry [27]. For the Pt-containing samples, two additional XRD peaks can be observed at high-angle values (i.e., 39.7 and 46.2° (2θ)). They can unambiguously be assigned to the d_{111} and d_{200} of platinum metal which means that during the oxidation of the organic templates ($C_{16}TMA^+$ and TX-100) an *in situ* platinum reduction from Pt^{IV} to Pt^0 occurs. As shown below by TEM analysis, this *in situ* reduction of platinum leads to the dispersion of metal particles in the Pt/MSU samples.

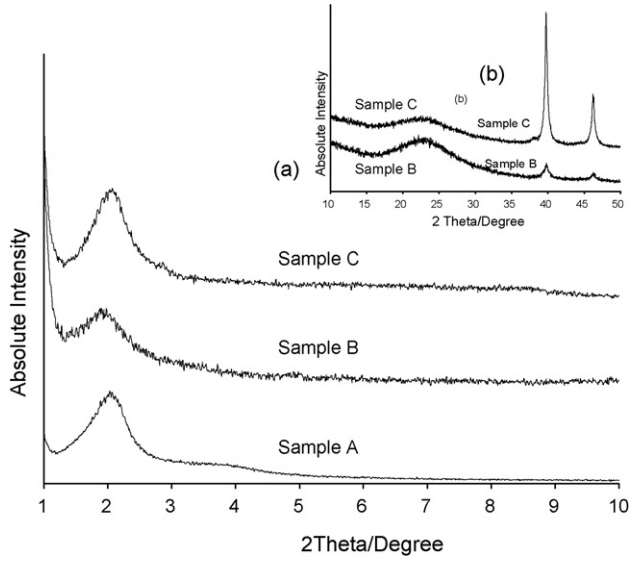

Fig. 1. Powder XRD patterns of the calcined Pt/MSU samples with various Pt loadings (sample A: (0 wt%), sample B: (1 wt%), sample C: (7 wt%)): (a) 2θ range 0–10° and (b) 2θ range 10–50°.

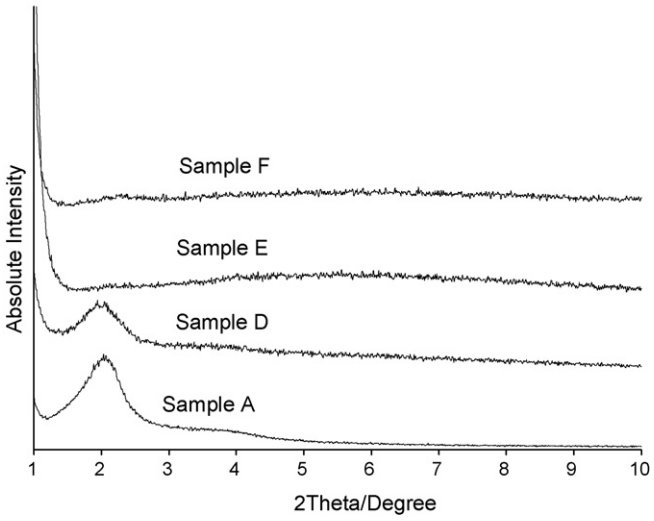

Fig. 2. Powder XRD patterns of the calcined HPW/MSU samples with various HPW loadings (sample A: (0 wt%), sample D: (9 wt%), sample E: (29 wt%) and sample F: (38 wt%)).

The XRD patterns of the calcined HPW/MSU samples with different HPW loadings (sample D (9 wt%), E (29 wt%) and F (38 wt%) are reported in Fig. 2. The XRD pattern of the lowest HPW-content sample (sample D) also exhibit a broad peak at $2\theta = 2°$ ($d = 44$ Å). However, an increase of the HPW loading (samples E and F) leads to the disappearance of this peak. Thus, as it was already reported for the HPW-containing SBA-3 materials [20], the incorporation of HPW strongly affects the long-range order of the structure.

For the Pt/HPW/MSU samples, a behavior similar to that described above for the HPW/MSU samples is observed. In that case too, for the calcined samples, XRD peaks corresponding to platinum metal with intensities in agreement with the Pt loading are present at high angle-values (XRD patterns not reported).

3.1.2. SEM

SEM micrographs of the calcined samples are reported in Fig. 3. All samples display a sphere-like morphology. Bigger particles are observed for the Pt-containing samples (samples B, C, G and I), the particles size ranging from 1 to 3 μm against 0.5 μm for pure silica sample (sample A). However, it is noteworthy that for the Pt/HPW/MSU samples, an increase of the HPW loading leads to a decrease of the particle size (compare samples G and J for instance) and the lost of the spherical morphology (sample J). These results are in good agreement with that obtained by Di Renzo et al. [28]. The authors suggested that the platinum salt, H_2PtCl_6, where platinum is forming anionic complex, induces extensive hydrolysis of TEOS. Monomeric silica species interact with the surfactant headgroups affording surfactant–inorganic complexes. If the condensation between siliceous units (Eq. (2)) is slower than the hydrolysis of the silica precursor (Eq. (1)), the rate of formation of nucleus able to grow, decreases, giving rise to larger particles, as observed by SEM for solids containing platinum (Fig. 3b and c). If the hydrolysis rate is low in comparison with condensation rate, the easy condensation between silanol groups on the surface of dif-

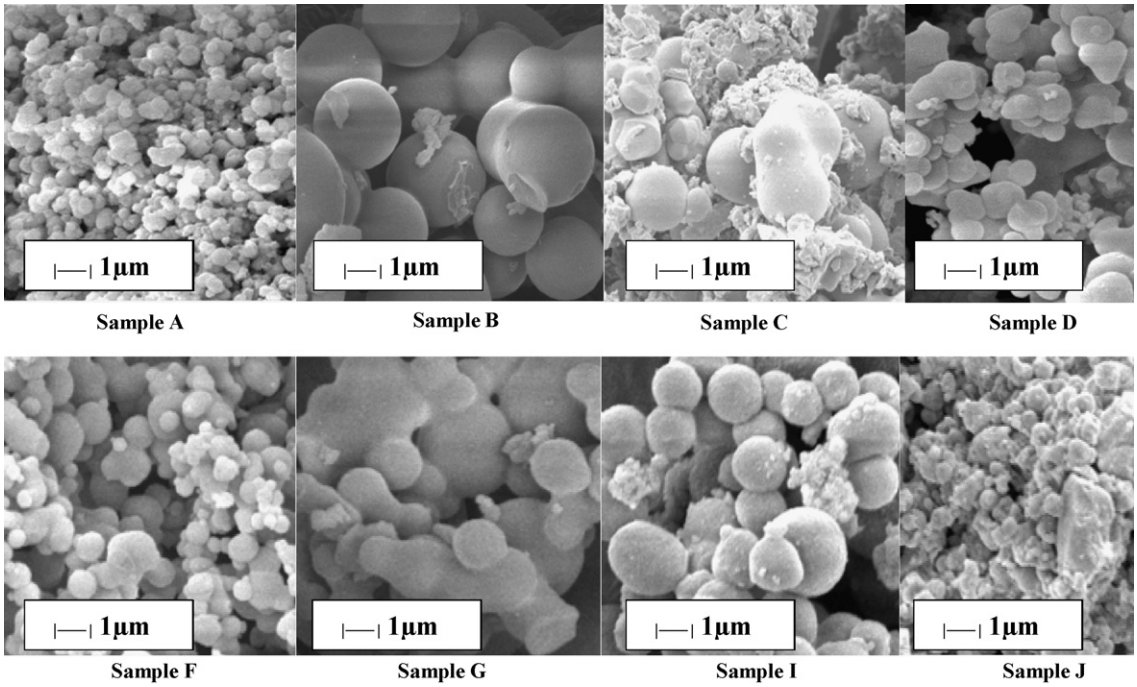

Fig. 3. SEM micrographs of calcined MSU (sample A), Pt/MSU (sample B: (1 wt%); sample C: (7 wt%)), HPW/MSU (sample D: (9 wt%); sample F: (38 wt%)) and Pt/HPW/MSU samples (sample G: Pt (0.5 wt%), HPW (13 wt%); sample I: Pt (0.3 wt%), HPW (22 wt%); sample J: Pt (0.8 wt%), HPW (49 wt%)).

ferent micelles brings about more rapid nucleation and therefore the formation of smaller particles (Fig. 3a) [28].

$$\equiv Si\text{–}OEt + H_2O \rightarrow \equiv Si\text{–}OH + Et\text{–}OH \quad (1)$$

$$\equiv Si\text{–}OH + HO\text{–}Si\equiv \rightarrow \equiv Si\text{–}O\text{–}Si\equiv + H_2O \quad (2)$$

3.1.3. Transmission electron microscopy

TEM analysis was performed on the Pt/and Pt/HPW/MSU materials (samples B, C, G, H, I and J). For the Pt/MSU samples, the TEM micrographs reveal the dispersion of quasi-spherical Pt particles in the siliceous matrix (Fig. 4). From the Gaussian distribution of the particle size a mean Pt particle size of 6.5 and 9.0 nm can be determined for sample B (1 wt% of Pt) and C (7 wt% of Pt), respectively. For the Pt/HPW-containing samples (samples G, H, I and J), although a lower Pt content (0.3–0.8 wt% of Pt), the particle size is larger and increases with the increasing of the HPW loading. In that case, the average particle size is close to 3.5, 7.4, 9.1 and 18.6 nm for samples G, H, I and J, respectively (Fig. 4). It is noteworthy that an increase of both the Pt and HPW loadings induces the broadening of the Pt particle size distribution.

3.1.4. Thermal analysis (TGA/DTA)

The thermal behavior of the as-synthesized MSU, Pt/MSU, HPW/MSU and Pt/HPW/MSU samples was investigated by TG/DTA thermal analysis (thermograms not shown). According to the nitrogen elemental analysis performed on these solids, only traces of $C_{16}TMA^+$ were present in all the as-synthesized materials; the main organic template being TX-100. For all samples, the TGA results are quite similar. A total weight loss of about 50 wt% occurs mainly in one step from 200 and 450 °C and is associated with at least three exothermic components on the DTA curve. These exotherms located at 200, 280 and 400 °C correspond to the oxidation of the organic template (TX-100). Indeed, the removal of TX-100 might be complete at 385 °C for 5 h (except samples with high HPW loading). Only the DTA curves for calcined samples, highly loaded with HPW, showed about 2% of the template remaining in the solid. Such a result has been reported before. Kluson et al. [29] showed that above 623 K, there was no existence for decomposed or partly decomposed poly(oxyethylene) chain (except molecular fragment with a mass of 205 or 206 as the prevailing component at 623 K extracted with toluene from the furnace). However, the authors did not mention the presence of a molecular fragment at 658 K, they suggest that the complete elimination of TX-100 would be better at 823 K.

3.1.5. BET and textural properties

For all samples the N_2 adsorption–desorption isotherms are of type IV with a capillary condensation step at around $P/P_0 = 0.3$–0.4 (Fig. 5). For clarity only isotherms of samples A, E and I are reported. The specific surface area (S_{BET}), pore volume and pore diameter determined from the adsorption branch of the isotherm using the BJH method are given in Table 2. For the Pt/HPW/MSU samples the condensation step occurs at a higher relative pressure (samples G and I) revealing a higher pore diameter. However the capillary condensation step is less steep (see sample I) which indicates a larger pore size distribution. As a general remark, the incorporation of Pt or HPW species leads, as expected, to a decrease of S_{BET} and the pore volume. For instance, they decrease from 1045 and 0.9 to 728 m^2/g and 0.5 cm^3/g when the amount of HPW increases from 9 to 38%, respectively (see Table 2, samples D, E and F). Except for the pore volume of sample H (pore volume = 0.97 cm^3/g), a similar

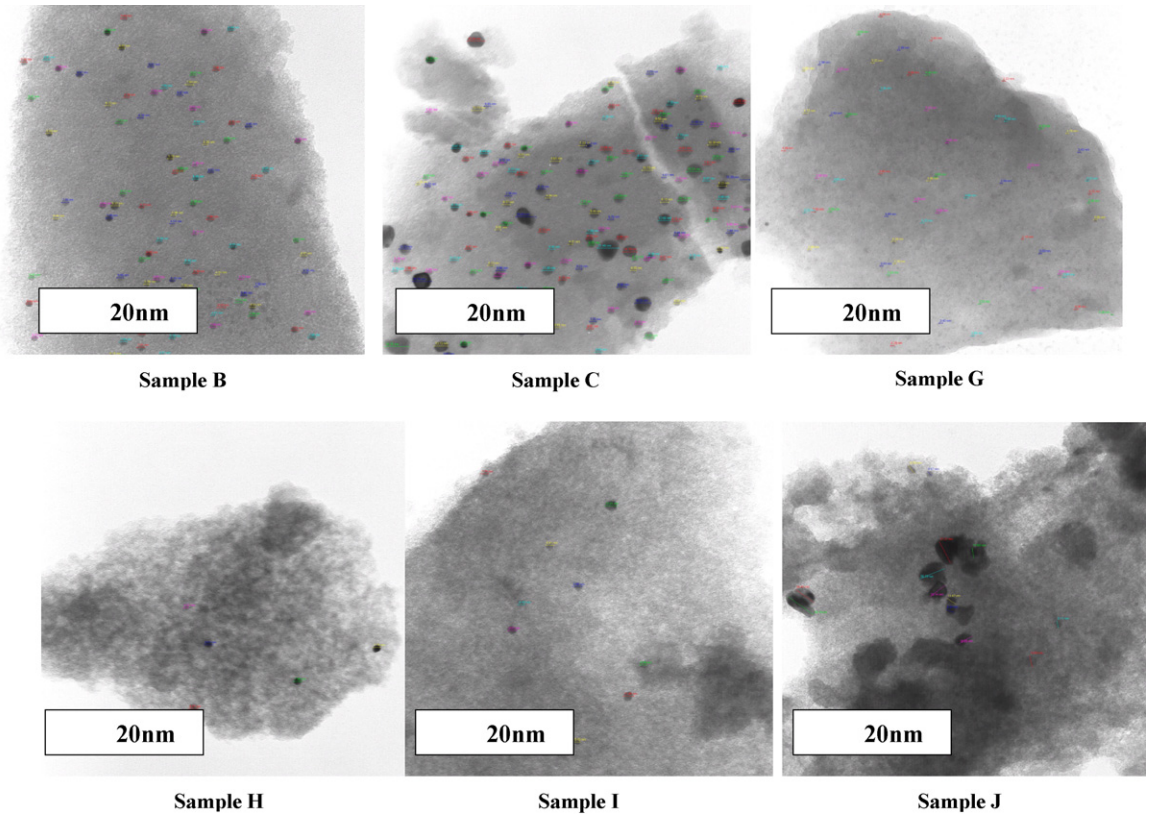

Fig. 4. TEM micrographs of the calcined Pt/MSU (sample B: (1 wt%); sample C: (7 wt%)), and Pt/HPW/MSU samples (sample G: Pt (0.5 wt%), HPW (13 wt%); sample H: Pt (0.4 wt%), HPW (20 wt%); sample I: Pt (0.3 wt%), HPW (22 wt%); sample J: Pt (0.8 wt%), HPW (49 wt%)).

trend is observed for the Pt/HPW/MSU samples; the decrease of S_{BET} being more pronounced (samples G, H and I). These results are in agreement with the XRD analysis. High Pt or HPW loadings strongly affect the characteristics of the samples, making structure disorder.

3.1.6. ^{31}P MAS NMR of HPW-containing samples

The as-synthesized and calcined HPW/MSU and Pt/HPW/MSU samples were characterized by ^{31}P MAS NMR. Whatever the sample, the as-synthesized materials display one resonance line at about −15.4 ppm (Fig. 6a). According to the literature, such a resonance can be assigned to hexahydrated HPW in which all polyanions are equally hydrogen bonded by $H_5O_2^+$ cations [30].

The ^{31}P MAS NMR spectra of the calcined HPW/MSU and Pt/HPW/MSU samples loaded with different HPW or Pt/HPW amounts exhibit several resonances between −16 and −12 ppm. For the HPW-containing samples (Fig. 6b, sample F) two main components at −15.2, −14.2 ppm are observed whereas for the Pt/HPW/MSU samples (G, H and I) four resonances at −15.3,

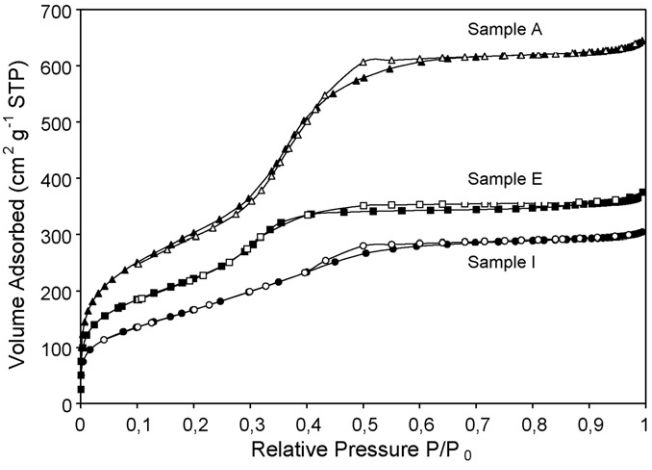

Fig. 5. N_2 adsorption (full symbols)–desorption (empty symbols) isotherms of MSU sample A, HPW/MSU sample E: HPW (29 wt%) and Pt/HPW/MSU sample I: Pt (0.3 wt%), HPW (22 wt%).

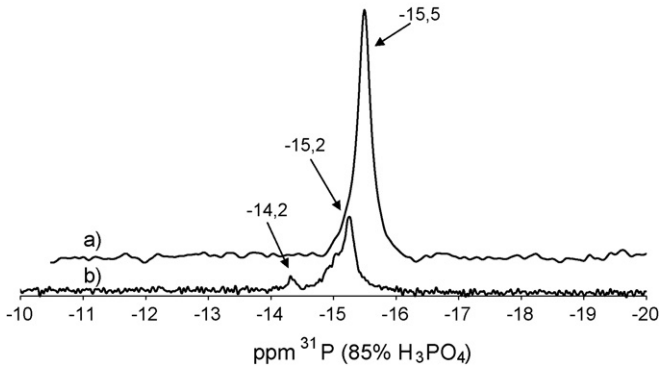

Fig. 6. ^{31}P MAS NMR spectra of the HPW/MSU sample F (38 wt%), as-synthesized (a) and calcined (b).

Table 2
Specific surface area, pore volume and pore diameter of the MSU, Pt/MSU, HPW/MSU and Pt/HPW/MSU samples

Sample	S_{BET}[a] (m^2/g)	V[a] (cm^3/g)	ϕ BJH[a] (Å)	S_{BET}[b] (m^2/g)	V[b] (cm^3/g)	ϕ BJH[b] (Å)
A	1104	0.99	27	–	–	–
B	1037	0.96	33–50	1015	0.99	33–50
C	927	0.55	25–40	595	0.39	25[c]
D	1045	0.91	26	962	0.72	27
E	828	0.56	27	712	0.41	27
F	728	0.49	25	270	0.28	25
G	941	0.94	35	830	0.53	25[c]
H	705	0.97	44[c]	683	0.79	44[c]
I	611	0.47	29[c]	408	0.30	29[c]
J	296	0.21	28[c]	304	0.22	28[c]

[a] Before catalytic tests.
[b] After catalytic tests.
[c] Broad distribution.

−14.4, −13.9 and −12.8 ppm are clearly detected (Fig. 7). Furthermore, an increase of the platinum content strongly affects the intensity of the component observed at −13.9 ppm; the higher the platinum loading, the higher the intensity.

In the calcined solids, the main component located at ∼−15 ppm corresponds to the hexahydrated HPW species. The ^{31}P MAS resonance lines from −12.5 to −14.4 ppm have already been observed in supported HPW/SiO_2 materials and were attributed to three types of species: (i) $[(SiOH_2)^+(H_2PW_{12}O_{40})^-]$ species arising from the interaction of HPW with the support surface [19]; (ii) HPW species differing in hydration levels [4,31,32]; and (iii) lacunary and/or dimeric species arising from a partial decomposition of HPW [30,33]. In the latter case, the decomposition could occur at the preparation stage, however it is not observed on the spectra of the as-synthesized materials (see Fig. 6a), or from its thermal degradation at high temperature starting around 400 °C [34], which cannot be totally excluded in our materials calcined at 385 °C.

According to solid-state ^{31}P NMR analysis, keggin units have been located in the bulk and on the surface of the support. Indeed the solid-state ^{31}P NMR spectrum displays two signals located at −15.3 and −14.6 ppm. Basing on the literature [35,36], the signal at −15.3 ppm has been attributed to HPW units that have no interaction with the silica support (in bulk), whereas the signal observed at −14.6 ppm has been assigned to the heteropolyanion in a slight interaction with the surface.

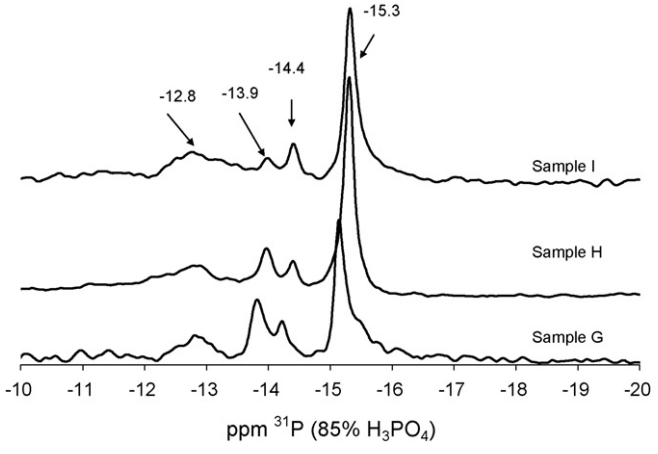

Fig. 7. ^{31}P MAS NMR spectra of calcined Pt/HPW/MSU samples with various Pt and HPW loadings (sample G: Pt (0.5 wt%), HPW (13 wt%); sample H: Pt (0.4 wt%), HPW (20 wt%) and sample I: Pt (0.3 wt%), HPW (22 wt%)).

However, some of these NMR components might also be assigned to the formation of complexes between HPW and Pt. Thus, according to Kuznetsova et al. [37], the formation of two types of complexes between Pt and $(PW_{11}O_{39})^{7-}$ was observed. The first one $[PW_{11}O_{39}Pt]$ showed a chemical shift at −13.2 and the second $[PW_{11}O_{39}Pt–O–PtPW_{11}O_{39}]$ at −12.8 ppm. The metal ions in the two complexes are connected with several (1–4) oxygen atoms located near the vacancy in the heteropolytungstate structure. Such a complex formation might explain the change observed in the intensity of the component at −13.9 ppm.

3.2. Catalytic properties

3.2.1. Catalytic reduction of NO_x over the HPW-containing samples

The conversion of NO_x over the HPW/MSU samples (D, E and F) loaded with various amounts of HPW (9, 29, and 38 wt%) was investigated between 170 and 350 °C and for an oxygen concentration between 0.5 and 10 vol.%. For all samples and whatever the O_2 concentration, the NO_x conversion level was very low (∼5%) when the temperature was below 250 °C. Above 250 °C, the NO_x conversion increased to reach about 20%.

At 300 °C (Fig. 8), the NO_x conversion increases when the oxygen concentration increases, and decreases when the HPW loading increases; the maximum of conversion does not exceed 20% in the best case for 10 vol.% O_2 with sample D containing the lowest amount of HPW (9 wt%). These results are compatible with the value indicated by Jentys et al. [11] who reported that the decomposition of NO_x over a 30 wt% HPW-loaded MCM-41-type catalyst was only 8% at 300 °C, but the oxygen concentration was not given. Actually, the NO_x conversion might be correlated to the specific surface area of the samples which decreases when the amount of HPW increases, the values being 1045, 828 and 728 m^2/g for samples D, E, and F, respectively (see Table 2).

In such catalysts, the HPW species are known to have a high capacity to adsorb polar molecules, especially NO_x, by substi-

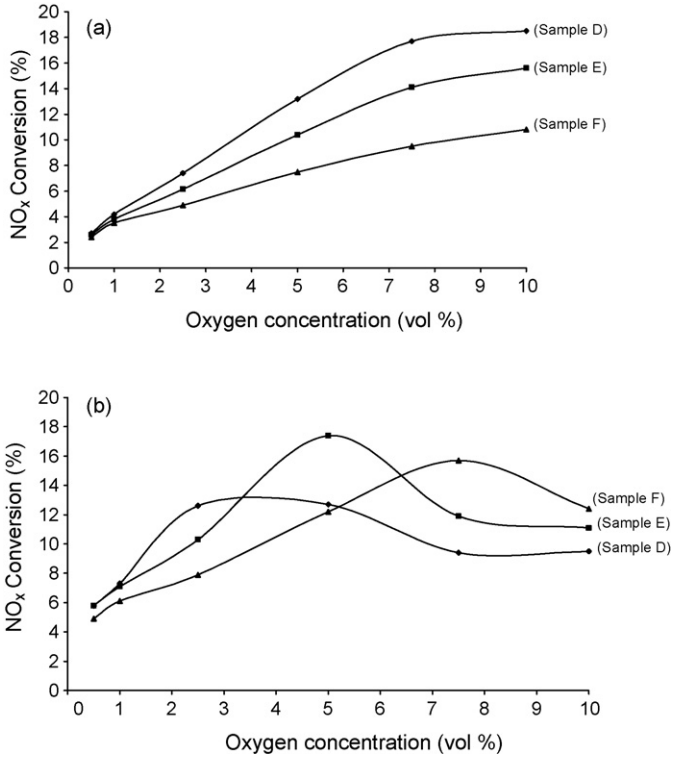

Fig. 8. Effect of oxygen concentration on the NO_x conversion at 300 °C (a) and 350 °C (b) over the MSU-type samples with different HPW loadings (sample D: (9 wt%), sample E: (29 wt%) and sample F: (38 wt%)).

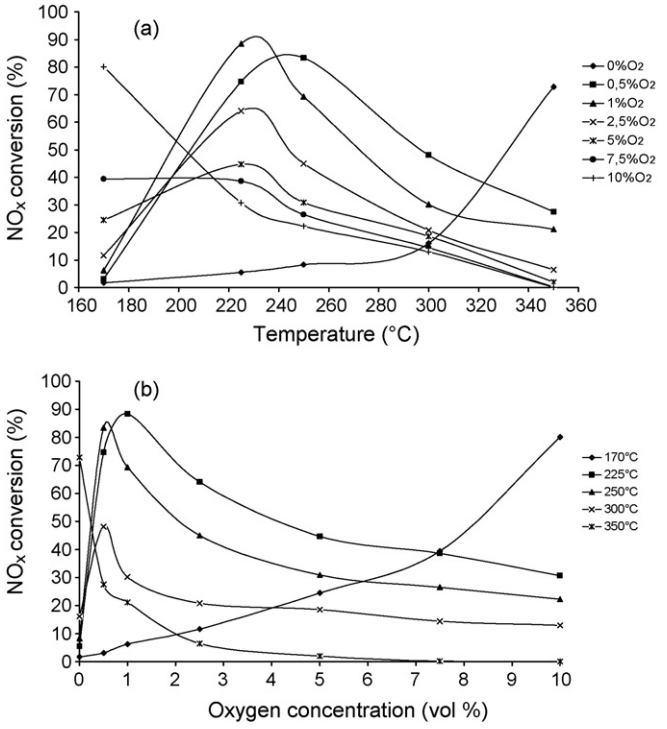

Fig. 9. Effect of temperature (a) and oxygen concentration (b) on the NO_x conversion over Pt/MSU sample (sample B: Pt (1 wt%)).

tution of the water occluded within their secondary structure [38]. Furthermore, it has been shown [38] that the adsorption of NO_2-free NO was impossible on HPW and that the adsorption capacity of NO reached a maximum of 46 mg per gram of HPW at 170 °C [39]. Moreover, McCormic et al. [40,41] reported that after the adsorption of NO_x over hydrated tungstophosphoric acid supported on SiO_2, protonated species were formed (i.e., NOH^+), which are almost completely decomposed (70–100% NO_x conversion) into N_2 and N_2O in the presence of O_2 and H_2O at 427 °C. The authors suggested a combined adsorption/decomposition mechanism, where tungstophosphoric acid adsorbs NO into its bulk structure as follows:

$$H_3PW_{12}O_{40} \cdot 6H_2O \overset{NO/O_2\,(150\,^\circ C)}{\longrightarrow} H_3PW_{12}O_{40} \cdot 3NO + 6H_2O$$

and subsequently a decomposition of NO into N_2 and O_2 occurs, according to:

$$H_3PW_{12}O_{40} \cdot 3NO \overset{H_2O/heat}{\longrightarrow} H_3PW_{12}O_{40} \cdot 6H_2O + (3/2)N_2 + (3/2)O_2$$

3.2.2. *Catalytic reduction of NO_x over the Pt-containing samples*

In spite of a significant porous volume and a high specific surface area, the previous tests showed that the catalytic activity of mesoporous silica containing only tungstophosphoric acid remains still small in deNO_x. Therefore, taking into account the well-known catalytic properties of platinum, especially in reduction reactions, Pt/MSU samples containing two amounts of Pt (1 wt% (sample B) and 7 wt% (sample C)) were tested between 170 and 350 °C and an oxygen concentration between 0 and 10 vol.%. For a small Pt loading, Fig. 9a and b shows the influence of temperature at a fixed amount of O_2 and the effect of oxygen concentration at a fixed temperature on the NO_x conversion, respectively.

In the absence of oxygen in the gas mixture, the NO_x conversion, which is very low at 170 °C (<3%) increases with increasing temperature, to reach about 73% at 350 °C (Fig. 9a). The concentration of C_3H_6 being set at 900 ppm at the reactor inlet, the critical oxygen concentration, defined as the stoichiometric oxygen concentration required for the complete oxidation of propene, is ca. 0.4 vol.%. Surprisingly, this value corresponds to the maximum conversion of NO_x for temperatures between 225 and 250 °C. The effect of O_2 concentration is very pronounced (Fig. 9b), thus, below the critical oxygen concentration, the conversion of NO_x increases and above this value, it decreases with increasing temperature. However at 170 °C, a different behavior is observed, the NO_x conversion increases with increasing oxygen concentration from 2% (0 vol.% O_2) up to 80% (10 vol.% O_2).

The role of oxygen which is found to be favorable at low temperature for the NO_x reduction over the Pt/MSU catalysts is believed to activate C_3H_6 to form oxidized hydrocarbon intermediates on the catalytic sites [42]. Those intermediates would react with NO_x adsorbed on the sites to lead to N_2 and N_2O. Thus, the curves (Fig. 9b) show that, in the absence of oxygen, the NO_x conversion is low when the reaction temperature is below 350 °C. With the increase of the O_2 concentration from 0 to 0.5–1 vol.%, the NO_x conversion is found to increase strongly.

For example, at 250 °C under 0.5 vol.% oxygen concentration, the NO_x conversion reaches about 85% for sample B. Because the temperature is not high enough for the complete oxidation of C_3H_6, the overall environment in the reaction mixture is still under reducing conditions, making possible the complete NO_x conversion. A maximum of conversion of 88% was observed at 225 °C under 1% of O_2. It has to be noted that at a temperature of 225 °C and above the conversion of C_3H_6 is always 100%.

Our results are comparable to those obtained by Shen and Kawi [43], Long and Yang [44] and Jentys et al. [11] who studied activity of Pt supported on MCM-41. The latter reported that over Pt-impregnated (1.6 wt%) MCM-41 at 240 °C, the NO_x conversion is very high (92%) for a low O_2 concentration (0.6 vol.%) and it decreases continuously with increasing O_2 concentration, for instance, 30% NO_x conversion was obtained for a O_2 concentration of 10 vol.%. In addition, the catalyst was found almost inactive in the absence of oxygen [44].

Similar observations are made for sample C containing 7 wt% of Pt. Without oxygen in the reaction mixture, the conversion of NO_x increases with increasing temperature, to reach about 78% at 350 °C. With 0.5 vol.% O_2, close to the critical oxygen concentration, the NO_x conversion reaches a maximum of about 97% at 225 °C and decreases with increasing temperature. Above the critical oxygen concentration, the conversion decreases slightly when the O_2 concentration increases and more strongly when the temperature increases.

3.2.3. Catalytic reduction of NO_x over the Pt- and HPW-containing samples

For clarity, only the results of NO_x conversion as a function of temperature for a fixed oxygen concentration, and as a function of oxygen concentration at constant temperature over the catalyst which contains a small amount of Pt and HPW (sample G) are shown in Fig. 10a and b, respectively. The maximum of NO_x conversion depends strongly on the temperature and on the oxygen concentration. Two series of maxima with high conversion values (>70%) are observed at 225 and 250 °C (Fig. 10a), corresponding to high concentrations of oxygen (>1%) and low ones (<2.5%), respectively. The highest NO_x conversion (96%) takes place at about 250 °C for low O_2 contents (0.5–1 vol.%) and is shifted towards 225 °C for high O_2 contents (2.5–10 vol.%). Fig. 10 shows that the catalyst is efficient in a large range of oxygen concentrations (0.5–10 vol.%), but for a narrow domain of temperature, i.e., between 225 and 250 °C.

The other samples containing similar Pt loadings but with higher HPW loadings show some similarities with those of sample G but with lower efficiency. The evolution of the maxima of NO_x conversion rates and optimal O_2 concentrations at both 225 and 250 °C are plotted versus HPW content in Fig. 11. The optimal O_2% concentration increases when the HPW loading increases. Whatever the temperature and considering a Pt content similar (0.5–1 wt%), the NO_x conversion rate is higher when a small amount of HPW (13 wt%, sample G) is introduced. It is noteworthy that in the presence of HPW, the NO_x conversion rate is higher at 250 °C. However, the increase in the HPW loading induces a decrease of the NO_x conversion rate.

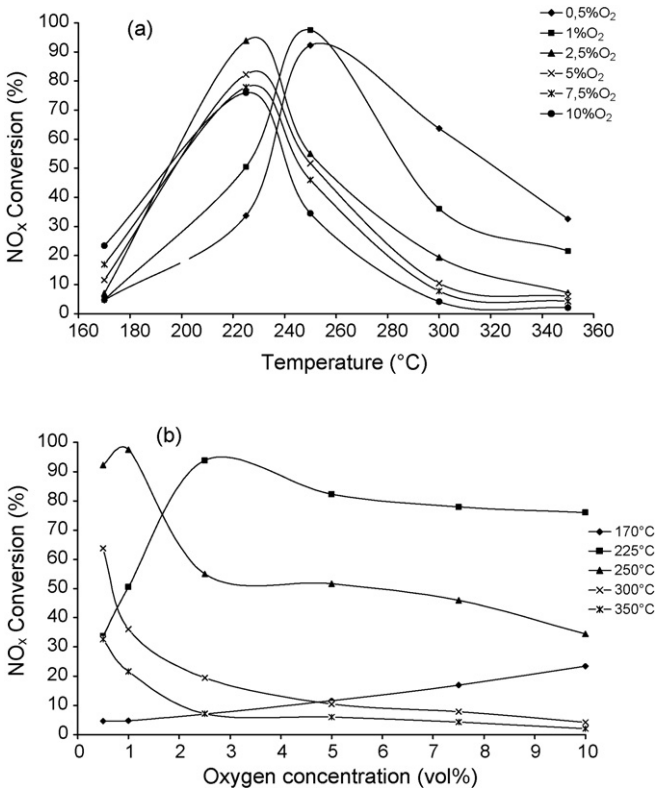

Fig. 10. Effect of temperature (a) and oxygen concentration (b) on the NO_x conversion over the incorporated Pt/HPW/MSU sample (sample G: Pt (0.5 wt%), HPW (13 wt%)).

3.2.4. Effect of water vapor on NO_x conversion

The effect of water vapor on the conversion of NO_x was determined on the most efficient catalyst (sample G: Pt (0.5% wt), HPW (13% wt)) and for one single temperature, i.e., 225 °C, which corresponds to the high levels of NO_x conversion for oxygen concentrations between 2.5 and 10 vol.%. Fig. 12 shows the effect of water vapor (2.5, 7.5 and 10 vol.% H_2O) on the NO_x conversion as a function of oxygen concentration. The con-

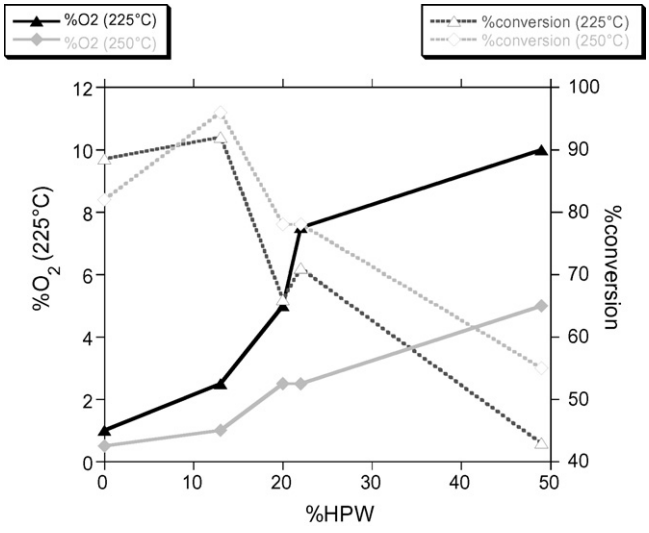

Fig. 11. Evolution of the maxima of NO_x conversion rates and optimal O_2 concentrations at both 225 and 250 °C vs. HPW content.

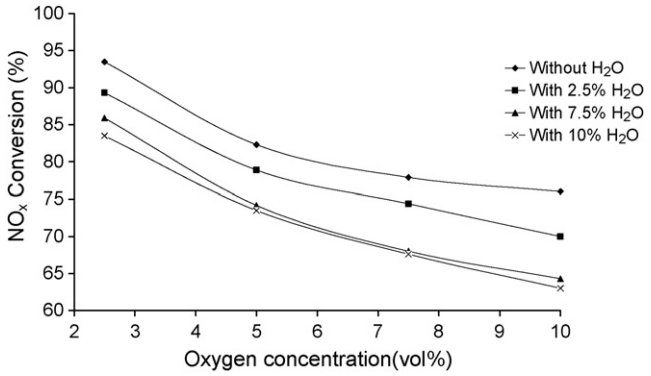

Fig. 12. Effect of water vapor on the conversion of NO_x at 225 °C over the incorporated Pt/HPW/MSU sample (sample G: Pt (0.5 wt%), HPW (13 wt%)).

version decreases as the oxygen concentration increases with or without water vapor. As an example, with 2.5 vol.% O_2, it decreases from 93 to 83% when the concentration of water vapor increases from 0 to 10 vol.%. This effect is slightly more pronounced for 10 vol.% O_2 and 10 vol.% H_2O. It has to be noted that the conversion of C_3H_6 is always 100% at 225 °C.

In order to study the ageing effect of the catalyst, on the NO_x conversion, in the presence or absence of water vapor, part of sample G was also treated under He containing 10 vol.% H_2O at 350 °C 4.5 h. The activity of the catalyst at 225 °C and with 10% vol. of O_2 before and after such a treatment is shown in Fig. 13. In the absence of water vapor, the NO_x conversion remains constant before and after ageing (∼76%). When the water vapor (10 vol.%) was introduced into the gas mixture, in both cases (before and after ageing), the NO_x conversion decreases from 76 to 63%, indicating that the negative effect of the water vapor is only observed during the catalytic reaction (Fig. 13). The decrease of NO_x conversion over the catalyst

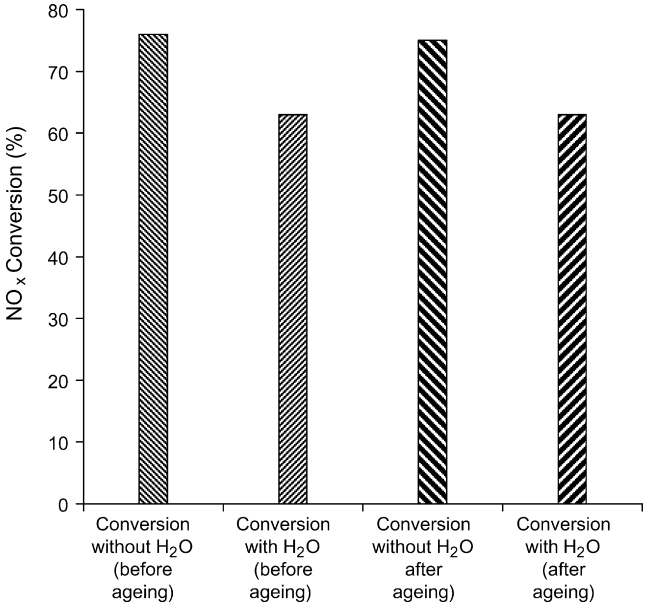

Fig. 13. Ageing effect on the conversion of NO_x in the absence or in presence of 10 vol.% of water vapor and O_2 (10 vol.%) at 225 °C over the incorporated Pt/HPW/MSU sample (sample G: Pt (0.5 wt%), HPW (13 wt%)).

(sample G) in the presence of this high concentration of water vapor might be attributed to the replacement of the adsorption of reactants on the catalyst surface by water molecules.

3.3. Characterization of the catalysts after deNO_x reaction

After catalytic tests, the XRD patterns of the Pt/MSU-, HPW/MSU- and Pt/HPW/MSU samples show no significant change. Especially, for samples B and C containing 1 and 7 wt% of platinum, respectively, the characteristic (1 1 1) and (2 0 0) lines of Pt metal are still present, and those corresponding to Pt oxide species are completely absent. For sample J containing 0.8 wt% Pt, the two lines appear very weakly, but for samples G, H and I, they are not visible as before the catalytic tests. In addition, for all HPW-containing materials, and especially for high HPW loadings, a poor organization of the mesoporous matrix is observed, but no additional loss of organization appears after the catalytic tests.

The nitrogen adsorption–desorption isotherms of the various solids after the catalytic tests indicate a more or less strong decrease of the BET specific surface area and pore volume (Table 2). This decrease of porosity might be partly attributed to the shaping operation of the catalysts (pelletization of samples at 80 MPa). In spite of a rather high wall thickness of about 18 Å, HPW-rich materials, such as sample F, would not be stable enough to resist to mechanical and hydrothermal treatments.

After catalysis, the ^{31}P MAS NMR spectra recorded on the various HPW- and Pt/HPW-containing samples show chiefly the same chemical shifts with a significant line near −15.5 ppm assigned to the hexahydrated HPW and other broader lines located between −13.7 and −12.0 corresponding to the HPW species interacting with the host material or differing in hydration levels. For samples containing a small amount of HPW a strong decrease (sample D) or the disappearance (sample G) of the main peak attributed to the hexahydrated HPW species is observed. TEM analysis was also performed on sample G after catalysis. The micrographs show no change of the dispersion and the size of the Pt particles.

4. Conclusion

In this study, a new way to directly incorporate Pt, HPW and Pt/HPW into MSU-type materials under acidic medium using cationic ($C_{16}TMA^+$) and neutral (TX-100) surfactants is described. The XRD patterns of the obtained solids reveal that the mesoporous structure is preserved when up to 7 wt% of Pt is introduced. Whereas, high HPW loadings (>20 wt%) strongly affect the long-range order of the MSU structure. Similar results are observed for the Pt/HPW/MSU materials.

During the calcination of the as-synthesized samples prepared in the presence of chloroplatinic acid, the oxidation of the organic templates leads to an *in situ* reduction of the platinum species (Pt^{IV} to Pt^0) which allows the dispersion of the metal particles. The analysis of the thermal decomposition of the organics which correspond mainly to TX-100 (only traces of $C_{16}TMA^+$ are detected) clearly shows that the decomposition occurs in

several steps and is acid catalyzed for the HPW-containing samples. As expected, the porous characteristics of the solids depend on the Pt and HPW loadings, the higher the loading; the more decrease the S_{BET} and pore volume. According to the ^{31}P MAS NMR results, a complex formation between Pt and HPW might be possible.

The HPW, Pt and HPW/Pt containing materials were tested in deNO_x catalysis. Indeed, it is well known that platinum and HPW have interesting catalytic properties, especially in deNO_x catalysis for platinum compounds. The advantage of using this type of mesoporous solids as support, results from its high surface area and narrow pore size distribution which allowed a homogenous dispersion of the heteropolyacid species and platinum particles.

The conversion of NO_x is moderate (∼20%) at 300 and 350 °C over the HPW/MSU-type samples. The Pt/MSU-type samples containing different amounts of platinum (1 and 7 wt%) show very high conversions (∼90%) which can only be reached when the concentration of oxygen is close to the critical oxygen concentration (∼0.5 vol.%) required for the stoichiometric oxidation of C_3H_6. Beyond this value, the activity decreases regularly with oxygen concentration.

Combining Pt and HPW leads to special and interesting features in NO_x catalysis. Thus, the Pt/HPW/MSU catalysts demonstrates high activity (between 60 and 90% conversion) for a small quantity of Pt (0.5 wt%) and moderate amount of HPW (∼15%) in the temperature range 225–250 °C and for a large oxygen concentration (0.5–10 vol.%). The maximum of NO_x conversion decreases, and is shifted to higher temperature when the amount of HPW increases. The effect of water vapor which was tested over a Pt/HPW/MSU material indicates a slight decrease of the catalytic activity, but the ageing of the catalyst under water vapor under moderate conditions did not affect its properties. After catalytic tests, the analysis of the samples by various techniques showed no/or very small change of the characteristics of the materials.

Acknowledgements

Thanks are due to Dr. L. Vidal for the TEM analysis and for the fruitful discussion. Financial support from the CEDRE bilateral program (No. 00Tsi F8/L21) is gratefully acknowledged.

References

[1] J.S. Beck, J.C. Vartuli, W.J. Roth, M.E. Leonowicz, C.T. Kresge, K.D. Schmitt, C.T.-W. Chu, D.H. Olson, E.W. Sheppard, S.B. McCullen, J.B. Higgins, J.L. Schlenker, J. Am. Chem. Soc. 114 (1992) 10834.
[2] R. Ryoo, S. Jun, J.M. Kim, M.J. Kim, Chem. Commun. (1997) 2225.
[3] A. Corma, Chem. Rev. 97 (1997) 2373.
[4] S. Damyanova, L. Dimitrov, R. Mariscal, J.L.G. Fierro, L. Petrov, I. Sobrado, Appl. Catal. A: Gen. 256 (2003) 183.
[5] A. Corma, V. Fornés, M.T. Navarro, J.J. Pérez-Pariente, J. Catal. 148 (1994) 1243.
[6] W. Schießer, H. Vinek, A. Jentys, Catal. Lett. 56 (1998) 189.
[7] J.-H. Jang, S.-C. Lee, D.-J. Kim, M. Kang, S.-J. Choung, Appl. Catal. A: Gen. 286 (2005) 36.
[8] J.Y. Jeon, H.Y. Kima, S.I. Woo, Appl. Catal. B: Env. 44 (2003) 301.
[9] A. Corma, A. Martinez, V. Martinez-Soria, J. Catal. 169 (1997) 480.
[10] S.-C. Shen, S. Kawi, Appl. Catal. B: Env. 45 (2003) 63.
[11] A. Jentys, W. Schießer, H. Vinek, Catal. Today 59 (2000) 313.
[12] U. Junges, W. Jacobs, I. Voight-Martin, B. Krutzsch, F. Schueth, J. Chem. Soc., Chem. Commun. (1995) 2283.
[13] N. Mizuno, M. Misono, J. Mol. Catal. 86 (1994) 319.
[14] I.V. Kozhevnikov, Catal. Rev. Sci. Eng. 37 (1995) 311.
[15] T. Okuhara, N. Mizuno, M. Misono, in: D.D. Eley, W.O. Haag, B. Gates (Eds.), Catalytic Chemistry of Heteropoly Compounds, vol. 41, Academic Press, San Diego, 1996, p. 113.
[16] Y. Izumi, R. Hasebe, K. Urabe, J. Catal. 84 (1983) 402.
[17] I.V. Kozhevnikov, Chem. Rev. 98 (1998) 171.
[18] M. Yoshimune, Y. Yoshinaga, T. Okuhara, Micropor. Mesopor. Mater. 51 (2002) 165.
[19] I.V. Kozhevnikov, K.R. Kloetstra, A. Sinnema, H.W. Zandbergen, H. van Bekkum, J. Mol. Catal. A 114 (1996) 287.
[20] K. Nowińska, R. Fórmaniak, W. Kaleta, A. Waclaw, Appl. Catal. A: Gen. 256 (2003) 115.
[21] D. Trong On, D. Desplantier-Giscard, C. Danumah, S. Kaliaguine, Appl. Catal. A: Gen. 253 (2003) 545.
[22] J. Jang, S.-C. Lee, D.-J. Kim, M. Kang, S.-J. Choung, Appl. Catal. A: Gen. 286 (2005) 36.
[23] J. Toufaily, Thèse Université de Haute Alsace, 2002.
[24] E. Prouzet, F. Cot, C. Boissière, P.J. Kooyman, A. Larbot, J. Mater. Chem. 12 (2002) 1553.
[25] S. Brunauer, P.H. Emmett, E. Teller, J. Am. Chem. Soc. 60 (1938) 309.
[26] P. Barrett, L.G. Joyner, P. Halenda, J. Am. Chem. Soc. 73 (1951) 373.
[27] S.A. Bagshaw, E. Prouzet, T.J. Pinnavaia, Science 269 (1995) 1242.
[28] F. Di Renzo, F. Testa, J.D. Chen, H. Cambon, A. Galarneau, D. Plee, F. Fajula, Micropor. Mesopor. Mater. 28 (1999) 437.
[29] P. Kluson, P. Kacer, T. Cajthaml, M. Kalaji, J. Mater. Chem. 11 (2001) 644.
[30] S. Uchida, K. Inumaru, M. Misono, J. Phys. Chem. B 104 (2000) 8108.
[31] V.M. Mastikhin, S.M. Kulikov, A.V. Nosov, I.V. Kozhevnikov, I.L. Mudrakovsky, M.N. Timofeeva, J. Mol. Catal. 60 (1990) 65.
[32] A. Ghanbari-Siahkali, A. Philippou, J. Dwyer, M.W. Anderson, Appl. Catal. A: Gen. 192 (2000) 57.
[33] L.R. Pizzio, C.V. Caceres, M.N. Blanco, Appl. Catal. A: Gen. 167 (1998) 283.
[34] P.A. Jalil, N. Tabet, M. Faiz, N.M. Hamdan, Z. Hussain, Appl. Catal. A: Gen. 257 (2004) 1.
[35] R. Thouvenot, M. Fournier, C. Rocchioccioli-Deltcheff, J. Chem. Soc., Faraday Trans. 87 (1991) 282.
[36] F. Lefebre, J. Chem. Soc., Chem. Commun. (1992) 756.
[37] N.J. Kuznetsova, L.G. Detusheva, L.I. Kuznetsova, M.A. Fedotov, V.A. Likholobov, J. Mol. Catal. A: Chem. I 14 (1996) 131.
[38] R. Bélanger, J.B. Moffat, J. Mol. Catal. A 114 (1996) 319.
[39] S. Hodjati, K. Vaezzadeh, C. Petit, V. Pitchon, A. Kiennemann, Top. Catal. 16/17 (2001) 151.
[40] A.M. Herring, R.L. McCormic, J. Phys. Chem. B 102 (1998) 3175.
[41] R.L. McCormic, S.K. Boonrueng, A.M. Herring, Catal. Today 42 (1998) 145.
[42] W. Schießer, H. Vinek, A. Jentys, Appl. Catal. B: Env. 33 (2001) 263.
[43] S.-C. Shen, S. Kawi, Catal. Today 68 (2001) 245.
[44] R. Long, R.T. Yang, Catal. Lett. 52 (1998) 91.